Electronic Supplementary Material (ESI) for Inorganic Chemistry Frontiers.

Supporting Information

An ultra-sensitive electrochemical sensor based on MOF-derived ZnO/Co_3O_4 decorated on graphene for low-level monitoring of α_1-AR antagonist alfuzosin in tablet and human samples

Gajapaneni Venkata Prasad, Venkatachalam Vinothkumar, Seung Joo Jang, Tae Hyun Kim*

Department of Chemistry, Soonchunhyang University, Asan, 31538, Republic of Korea

*Corresponding author: Prof. Tae Hyun Kim (E-mail: thkim@sch.ac.kr)

Table of Contents

1. Materials and Methods

S1. Chemicals

Alfuzosin hydrochloride (AFZ), Ascorbic acid (AA), Uric acid (UA), dopamine (DA), tyrosine (TY), and folic acid (FA), Cobalt nitrate hexahydrate ($Co(NO_3)_2.6H_2O$), Zinc nitrate hexahydrate ($Zn(NO_3)_2.6H_2O$), 2-methylimidazole (2-MIM), Glucose ($C_6H_{12}O_6$), potassium hydroxide (KOH), human serum, sodium dihydrogen phosphate (NaH_2PO_4), and disodium hydrogen phosphate (NaH_2PO_4) were obtained from the Sigma-Aldrich (United States). Methanol was purchased from SK Chemicals, Republic of Korea. Graphene sheets were obtained from Acros Organics and the tablet sample (ALFOO-10 mg) was purchased from the local pharmaceuticals in Asan, Republic of Korea. All the compounds were utilized without any purification.

S2. Instrumentations

The powder X-ray diffraction (XRD) apparatus (MPD for bulk, 3KW, PANalytical) was used to assess the phase purity and crystal structure of the as-synthesized catalysts using monochromatic high-intensity Cu Kα radiation (1.5406 A^o). The Attenuated Total Reflectance-infrared (ATR-IR) spectra of all produced catalysts were obtained using a Thermo NICOLET iS5, iD5 ATR spectrometer (United States). The X-ray photoelectron microscopy (XPS) apparatus (Kratos, AXIS Supra, Manchester, UK) validated the binding energies of Co 2p, Zn 2p, O 1s, and C 1s molecules in the produced ZnO/Co_3O_4@Gr using a monochromatic Al-K X-ray source (15 kV, 375W). Surface morphology and microstructural investigation of as-synthesized materials were performed using a field emission scanning electron microscope (FE-SEM, JSM-7800F) JEOL Ltd, Japan. The more detailed microstructural properties were studied by field emission transmission electron microscope (FE-TEM, JEM-F200 (TFEG)) JEOL Ltd, Japan.

S3. Electrochemical measurements

The electrochemical measurements were performed through cyclic voltammetry (CV), differential pulse voltammetry (DPV), and Electrochemical impedance spectroscopy (EIS) studies using a CHI 760E (USA) electrochemical analyzer. A standard three-electrode setup with ZnO/Co_3O_4@Gr/GCE, Pt-wire, and saturated calomel electrode (SCE) served as working, counter, and reference electrodes, respectively. A potential range of 0.4 V to 1.2 V and a scan rate of 100 mV/s were used to evaluate the electrochemical oxidation reaction of AFZ with 0.1 M PBS as an electrolyte.

S4. Preparation of real samples

In order to prepare the AFZ tablet sample solution, 10 mg of AFZ tablet that is accessible on the local pharmaceuticals was purchased. To achieve the calibration range of standard AFZ, the tablet was crushed into a fine powder using an agate mortar and dissolved in 100 mL of 0.1 M PBS (pH 7.0). After thoroughly shaking the solution to the desired concentration, it was utilized to analyze. The samples of human serum were collected and stored in a refrigerator. Prior to the experiment, the serum samples were diluted ten times in 0.1 M PBS (pH 7.0). The human urine sample was taken from the healthy volunteer and preserved in the refrigerator. A suitable volume of urine was collected before measurement and centrifuged at 10000 rpm for 15 min to prepare a test solution.

2. XRD patterns of as-prepared ZIFs

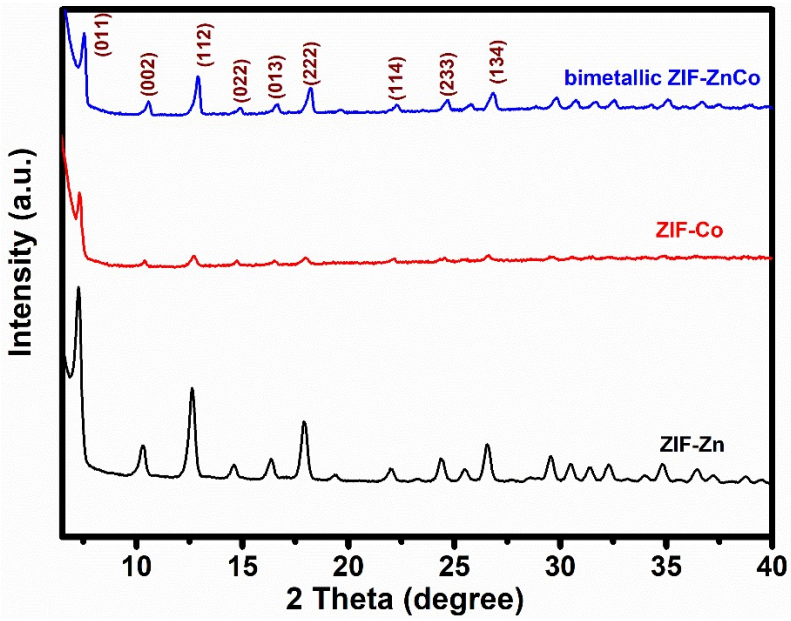

Fig. S1. XRD patterns of ZIF-Zn, ZIF-Co, and bimetallic ZIF-ZnCo.

3. ATR-IR spectra of as-prepared ZIFs and their oxides

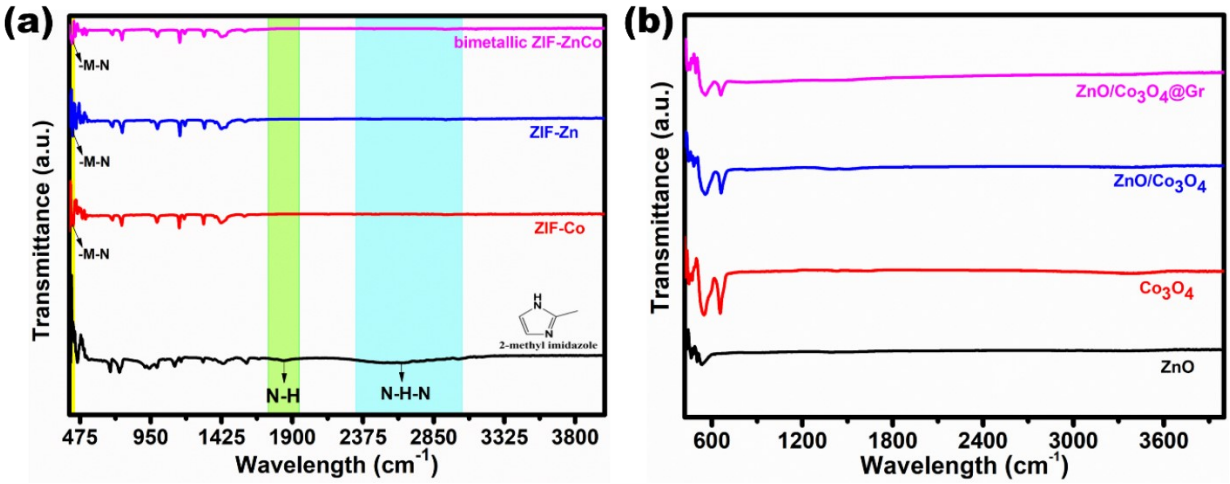

Fig. S2. ATR-IR spectra of (a) 2-methyl imidazole, ZIF-Co, ZIF-Zn, and bimetallic ZIF-ZnCo, (b) ZnO, Co_3O_4, ZnO/Co_3O_4 and ZnO/Co_3O_4@Gr, respectively.

4. FE-SEM images of as-prepared ZIFs with EDS analysis of bimetallic ZIF-ZnCo

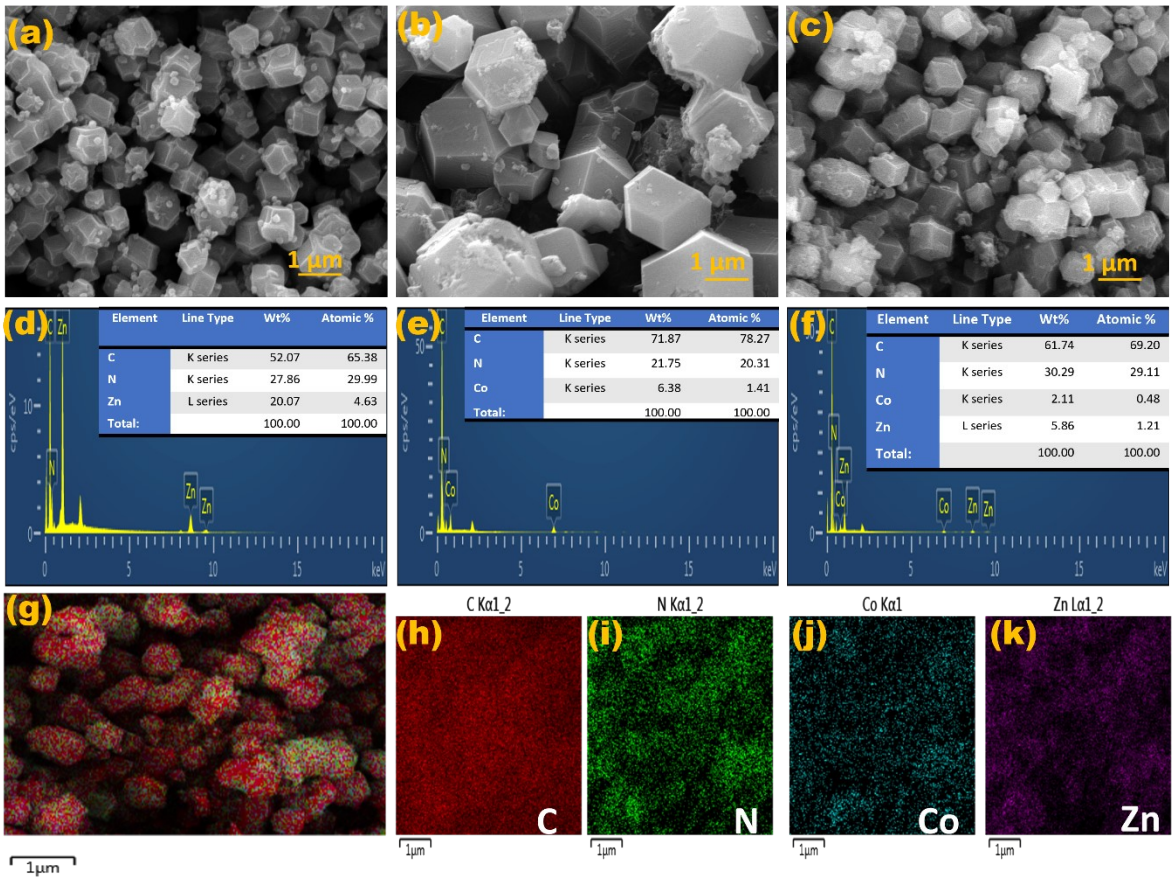

Fig. S3. FE-SEM images of (a) ZIF-Zn, (b) ZIF-Co, and (c) bimetallic ZIF-ZnCo. EDS spectrum of (d) ZIF-Zn, (e) ZIF-Co, and (f) bimetallic ZIF-ZnCo, respectively. (g–k) EDS mapping analysis of the bimetallic ZIF-ZnCo.

5. EDS analysis of ZnO, Co_3O_4, and ZnO/Co_3O_4 composite

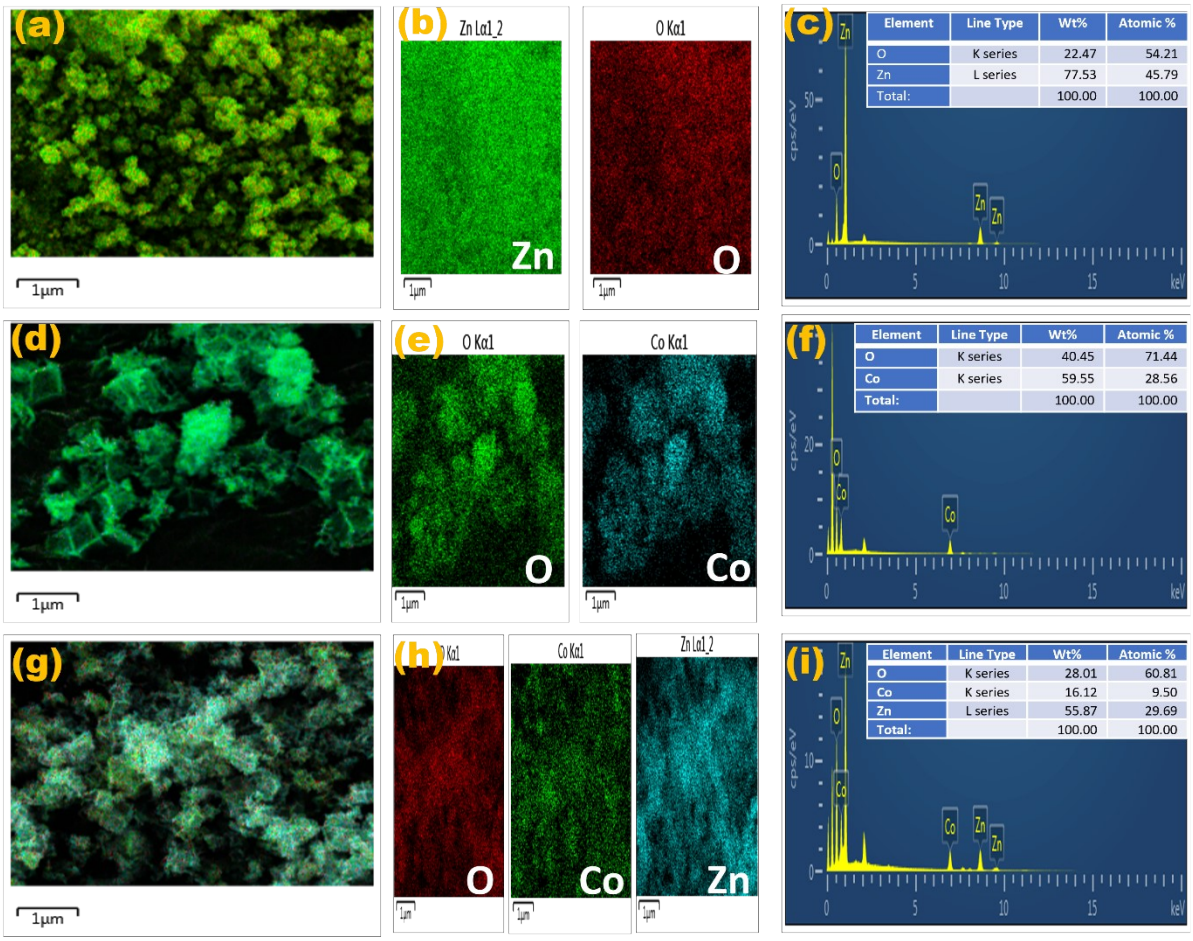

Fig. S4. (a–c) EDS mapping and spectrum of ZnO, (d–f) EDS mapping and spectrum of Co_3O_4, and (g–i) EDS mapping and spectrum of ZnO/Co_3O_4 composite.

6. Scan rate effects of various modified electrodes in the redox probe $[Fe(CN)_6]^{-3/-4}$

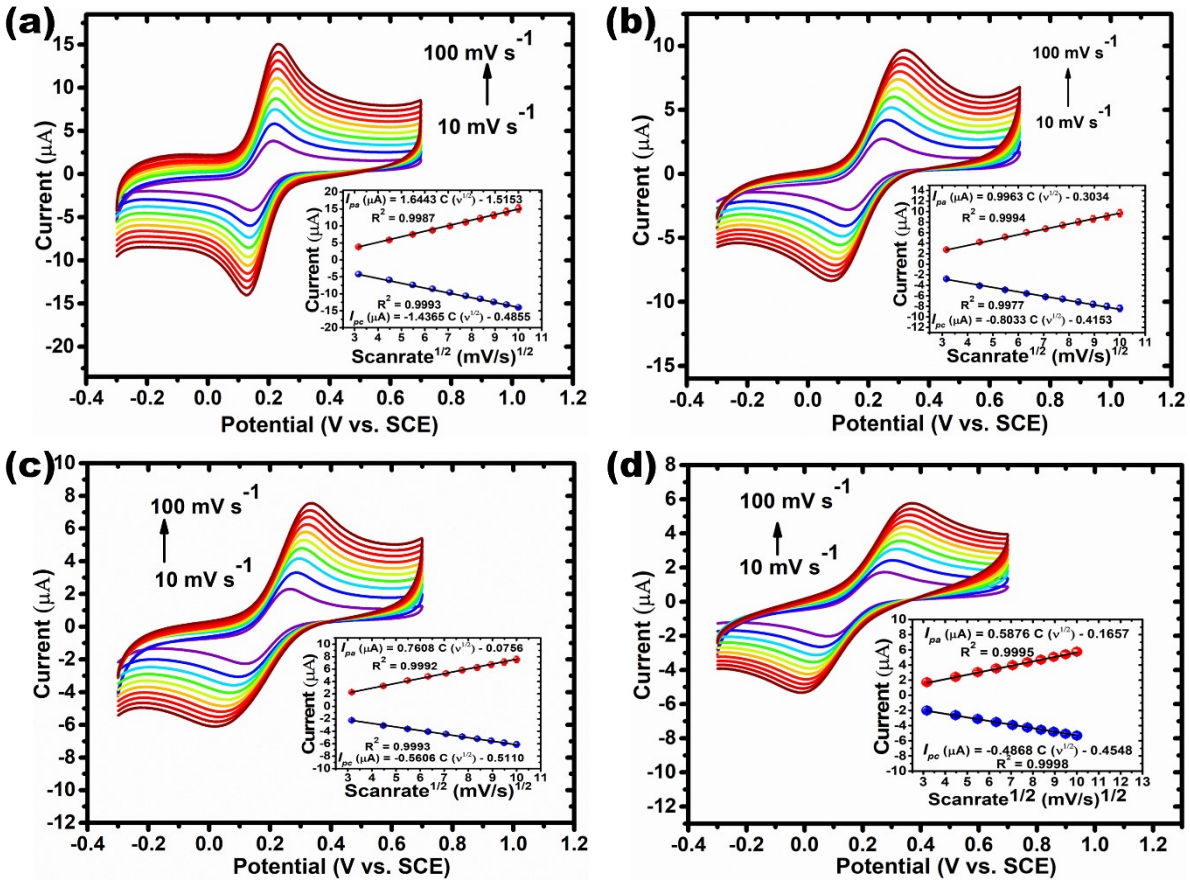

Fig. S5. (a) CV curves of Gr/GCE at various scan rates ranging from 10 to 100 mVs^{-1}. Inset: Calibration plot for $\upsilon^{1/2}$ vs. peak currents (I_{pa}/I_{pc}). (b) CV curves of ZnO/Co_3O_4/GCE at various scan rates ranging from 10 to 100 mVs^{-1}. Inset: Calibration plot for $\upsilon^{1/2}$ vs. peak currents (I_{pa}/I_{pc}). (c) CV curves of Co_3O_4/GCE at various scan rates ranging from 10 to 100 mVs^{-1}. Inset: Calibration plot for $\upsilon^{1/2}$ vs. peak currents (I_{pa}/I_{pc}). (d) CV curves of ZnO/GCE at various scan rates ranging from 10 to 100 mVs^{-1}. Inset: Calibration plot for $\upsilon^{1/2}$ vs. peak currents (I_{pa}/I_{pc}).

7. Electrochemical behavior of AFZ at modified electrodes

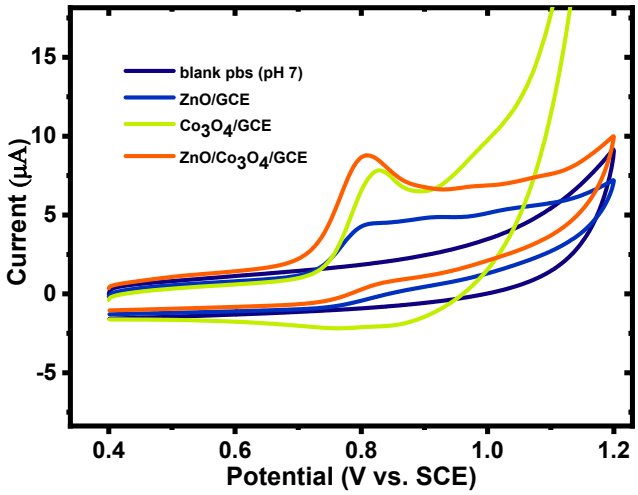

Fig. S6. CV curves of ZnO/GCE, Co_3O_4/GCE, and ZnO/Co_3O_4/GCE electrodes in PBS with pH 7.0 in the presence and absence of 1mM AFZ at a scan rate of 100 mVs^{-1}.

Sample	Added (µM)	Found (µM)	Recovery (%)	Bias (%)
ALFOO Tab	5	4.96	99.20	−0.8
	10	9.89	98.90	-1.1
	15	14.96	99.73	−0.27
Human urine	5	4.93	98.60	−1.4
	10	9.94	99.40	−0.6
	15	14.93	99.53	−0.47
Human serum	5	4.98	99.60	-0.4
	10	9.88	98.80	-1.2
	15	14.58	97.20	-2.8

8. The analysis results of AFZ in real samples at ZnO/Co_3O_4@Gr/GCE

Table S1: Determination of AFZ in real samples based on the proposed ZnO/Co_3O_4@Gr/GCE.